PROCEEDINGS OF SCIENCE

# Study of potential the observables for Gamma/Hadron separation in the SWGO observatory

**T. Capistrán*** **on behalf of the SWGO Collaboration**

*Università degli Studi di Torino, I-10125 Torino, Italy*
*INFN, Sezione di Torino, Torino, Italy*
*E-mail:* tomas.capistranrojas@unito.it

A significant challenge encountered by ground-based gamma-ray observatories is the substantial quantity of cosmic-ray particles that trigger detections. Therefore, it is crucial to implement techniques that can distinguish and separate gamma-ray showers from cosmic-ray showers. The Southern Wide-field Gamma-ray Observatory (SWGO) will be an array of water Cherenkov detectors, currently planned for construction in Chile in the Southern Hemisphere. The current simulation of the observatory includes a set of parameters as potential observables, some of which have demonstrated strong potential for effective Gamma/Hadron separation. In this work, we present an analysis of the performance of the most promising of these observables under different ranges of reconstructed energy, core position, and arrival direction.

39th International Cosmic Ray Conference (ICRC2025)
15–24 July 2025
Geneva, Switzerland

*Speaker



https://pos.sissa.it/

PoS(ICRC2025)593

## 1. Introduction

Successful high-energy source detection using indirect methods is dominated by arrays of Imaging Atmospheric Cherenkov Telescopes (IACTs), which provide excellent sensitivity and good separation between the cascades generated by gamma rays or hadrons [1]. Later, a different and complementary observational technique was developed: water Cherenkov detectors, such as HAWC [2] and LHAASO [3]. In fact, HAWC has discovered several new sources, as reported in the second and third catalogs [4, 5], and has demonstrated the ability to monitor them [6], among other capabilities. Like IACTs, this kind of observatory must implement gamma/hadron separation during the source analysis phase.

The most traditional and simple way to distinguish between two species is to apply dedicated cuts to observables. In the case of HAWC, two observables (Parameter for Identifying Nuclear Cosmic-rays, PINC, as described in Section 3, and Logarithm Inverse of the Compactness[1], `LIC`) [7] are used to remove the hadron contribution from the data when analyzing gamma-ray sources. Recent advances in the field of artificial intelligence, particularly in machine learning and deep learning, have enabled the implementation of techniques that achieve excellent results in classification and reconstruction tasks. Gamma/hadron separation is a perfect example of a classification problem. HAWC and LHAASO have begun to explore these kinds of techniques, implementing a multi-layer perceptron (MLP) [7, 8], which combines several observables to predict the type of particle detected. Since the event data recorded by these observatories consist mainly of a matrix of photomultiplier tubes (PMTs), which can be interpreted as an image, deep learning models have also been explored [9–11].

The Southern Wide-field Gamma-ray Observatory (SWGO) will be a ground-based experiment installed in Pampa La Bola, Chile, at an altitude of 4,770 meters. SWGO will consist of an array of water Cherenkov detectors (WCDs) distributed across three regional zones: a central zone with the highest density of WCDs (with a fill factor, FF, of approximately 65–75%), and intermediate and outer zones with decreasing WCD density (with FFs of 4% and 1.7%, respectively)[2]. Since the establishment of the SWGO collaboration in 2019, one of the main efforts has focused on creating observables that help distinguish between gamma and hadron events. One approach has involved training and implementing a graph neural network (`GNN`) to identify patterns in the data for event classification [11].

Currently, SWGO analyses use a `MLP` to combine all the gamma/hadron separation information and produce a single value indicating the particle type. In this contribution, we present an analysis aimed at identifying the most relevant parameters for the gamma/hadron separation task, which are then used as input to the `MLP` model, as reported in Section 4. The description of these observables is provided in Section 3, and the data used is described in Section 2. Section 5 summarizes the results of this contribution.

[1] Where compactness is defined as the number of PMTs with charge during an event over the maximum charge far (> 40 m) from the shower core.

[2] See Figure 2 in [12] to visualize these regional zones.

## 2. SWGO data

The simulation of SWGO data is based on that of HAWC. First, the extensive air shower is simulated using CORSIKA; then, the interaction between secondary particles and the detector is simulated with HAWCSim [13]; finally, the events are reconstructed using the charge and time collected from each PMT [12]. An alternative simulation method, optimized for very high energies (>100 TeV), is known as "fast simulation." This approach uses a parametrization of the signal detected in the WCDs, making it more efficient in terms of computing time [14]. The data used in this contribution were generated using this fast simulation method. The data were grouped into five logarithmic energy bins from 4.5 to 7.0, with a step of 0.5; three core position bins: central, intermediate, and outer[3]; and three zenith angle bins: vertical (0°–30°), moderate (30°–45°), and horizontal (45°–52°) events. There are 45 bins in total; however, in this procedure, we analyze only the 15 bins corresponding to vertical events across all logarithmic energy and core position bins. A quality cut is applied, requiring successful reconstruction of energy, core position, and direction.

## 3. Gamma/hadron separation observables

The reconstructed files generated by the fast simulation contain diverse information, such as energy estimators, core position, arrival direction, several gamma/hadron separation observables, and a fit of the lateral distribution function (LDF) using the NKG equation. Some observables originate from the HAWC observatory but have been optimized for the characteristics of the SWGO detector. For example, the `PINC` quantifies the evenness of the lateral charge distribution function [13], and `LDFChi2` represents the chi-square value from the LDF fit [7]. Other observables were developed by the SWGO collaboration, such as `LCm`, which evaluates fluctuations in the WCD signal at the azimuthal level [15]; and variables related to the quality of the angle and energy fits, `AFQ` and `LHQ`. Additionally, two observables based on deep learning models have been implemented. Both models use WCD information, charge and time, as input and compute a value between 0 and 1 to predict the primary particle type (gamma or hadron). These models differ in architecture: one uses Graph Neural Networks (`GNNs`) [11, 16], while the other, Deep learning for Extensive Air Shower Targeted Event Reconstruction (`DeepEASTER`), employs an attention-based neural network [17]. These are not the only available observables in the reconstruction; however, we focus on those with the highest gamma/hadron separation power in order to provide a reduced input list for the `MLP`, leading to improved classification performance.

## 4. Analysis & results

The goal of the gamma/hadron separation task is to retain the largest possible fraction of gamma events while rejecting as many hadron events as possible. A typical metric used in high-energy astrophysics to quantify the separation between them is the Q factor. It is defined as: $Q = \epsilon_g/\sqrt{\epsilon_p}$, where $\epsilon_g$ is the fraction of gamma events correctly classified (called gamma efficiency), and $\epsilon_p$ is the fraction of proton events misclassified (proton efficiency)[4].

[3] Same three regional zones in SWGO.

[4] Although this is typically referred to as hadron efficiency, in this work only proton events are employed; for this reason, we refer to it specifically as proton efficiency.



PoS(ICRC2025)593

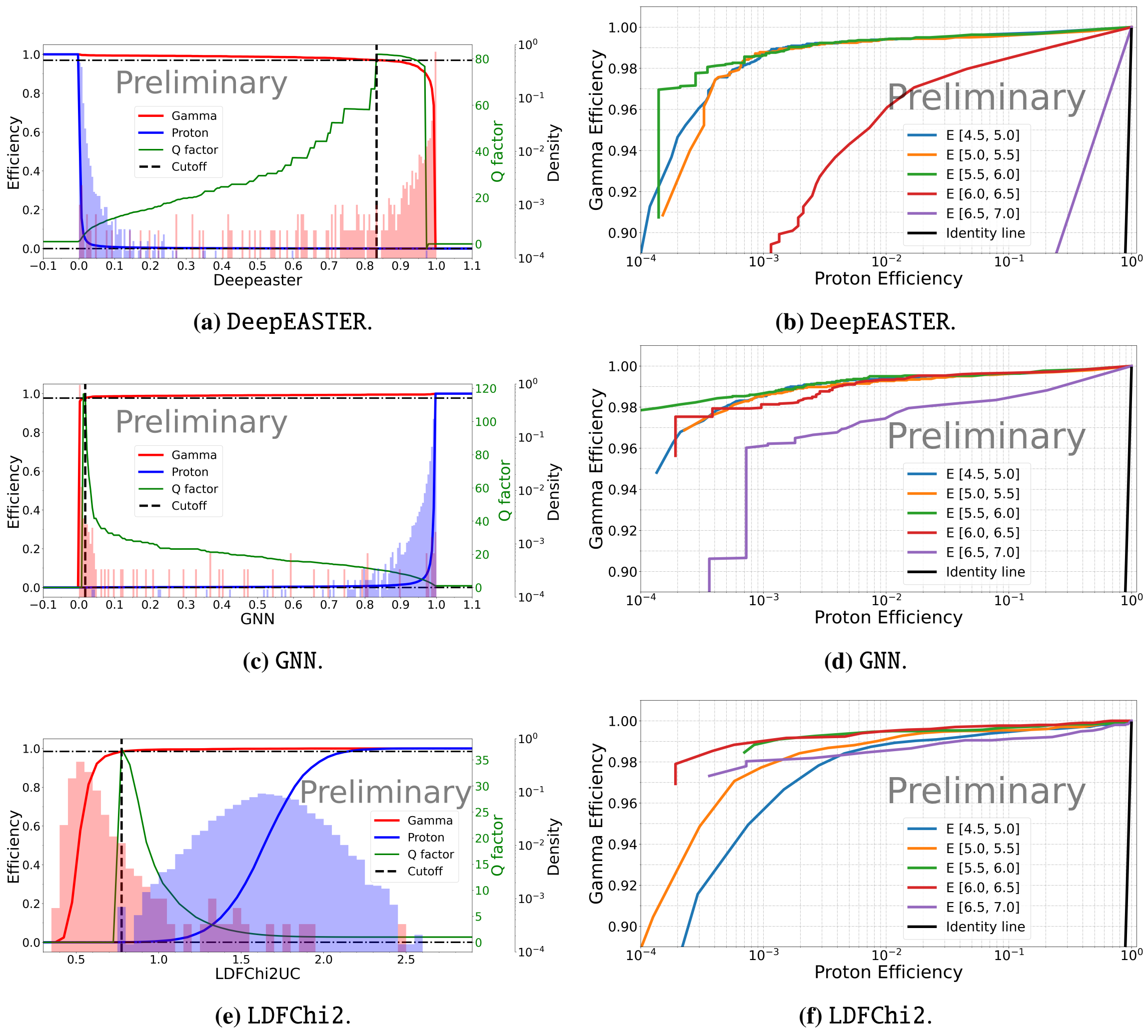


**(a)** `DeepEASTER`. **(b)** `DeepEASTER`.

**(c)** `GNN`. **(d)** `GNN`.

**(e)** `LDFChi2`. **(f)** `LDFChi2`.

**Figure 1:** The performance of the `DeepEASTER`, `GNN`, and `LDFChi2` observables is presented. The Figures in the left column show the distributions of these observables for gamma and proton events, along with their corresponding gamma efficiency, proton efficiency, and Q-factors, represented by the red, blue, and green lines, respectively. The events used have logarithmic energies between 5.5 and 6.0 and the intermediate core bin. The Figures in the right column display the ROC curves for these observables across five different energy bins, using events within the same zenith angle and core position ranges as those in the Figures on the left.

An independent performance analysis was conducted for each bin across all observables in the reconstruction list. This process allowed us to identify which observables offer the most effective gamma/hadron separation. The selected observables exhibit minimal overlap between the gamma and proton event distributions. This pattern is shown in the left column of the Figure 1, where histograms of three observables are presented for a specific bin corresponding to the intermediate core region and logarithmic energies between 5.5 and 6.0. Additionally, these Figures display the gamma and proton efficiencies and Q factors at different thresholds. The optimal cutoff is defined as the threshold yielding the maximum Q factor, subject to the condition that the gamma efficiency is greater than 80%. The efficiency information is used to build the Receiver Operating Characteristic (ROC) curves shown in the right column of Figure 1. The ROC curves provide a visual representation of the correlation between gamma and hadron efficiencies. The best classifier corresponds to the curve closest to the top-left corner of the figure[5]. Observables with curves closest to this point are selected as the best classifiers.

The figures in the right column illustrate the behavior of three observables across different logarithmic energy bins within the intermediate core bin. It is important to note that the separation power of these observables varies across energy bins. Better separation is achieved at higher energies, where more WCDs typically participate in the detection footprint, providing richer information for event reconstruction. Despite this energy dependence, these observables offer the best gamma/hadron separation performance across the full energy range of SWGO. A similar trend is observed across the core bins. The observables exhibit different separation performance depending on the core location, with the best results obtained for events whose cores are located near the center of the array. This is because central events are almost fully detected, providing more complete information for reconstruction (see Figure 2).

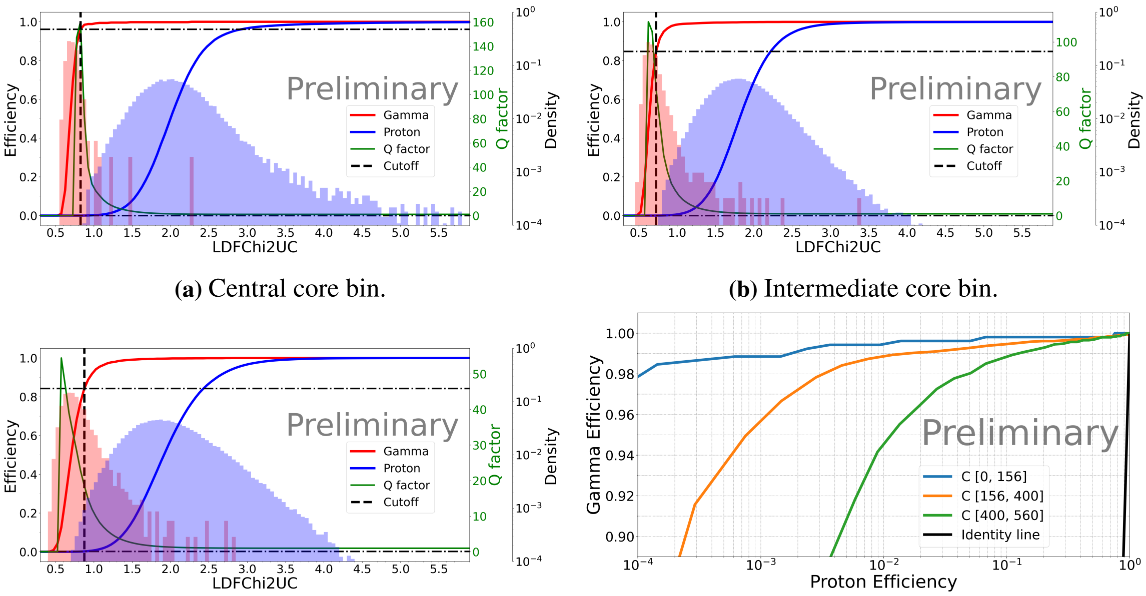


**(a)** Central core bin.

**(b)** Intermediate core bin.

**(c)** Outer core bin.

**(d)** ROC curves.

**Figure 2:** The performance of the `LDFChi2` observable is shown for three different bins corresponding to the central (a), intermediate (b), and outer (c) core bins, using the same colors and line definitions as in Figure 1. The events have energies between 4.5 and 5.0 (logarithmic scale). In (d), the ROC curves for this observable across these three core bins are presented, demonstrating good overall performance with distinct behaviors in each.

After optimizing the selection of observables for this classification task, all this information can be combined to obtain better results. To achieve this, a `MLP` was trained. This model was fed with

[5]This point represents the optimal classification, where the model correctly classifies all events, regardless of particle type.

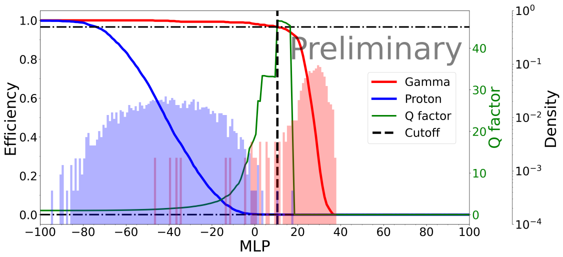


**(a)** Central core bin.

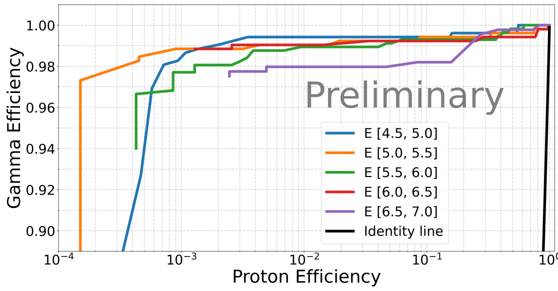


**(b)** Central core bin.

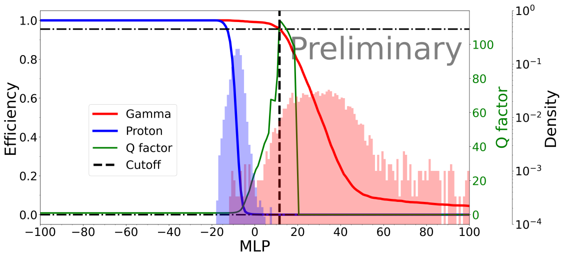


**(c)** Intermediate core bin.

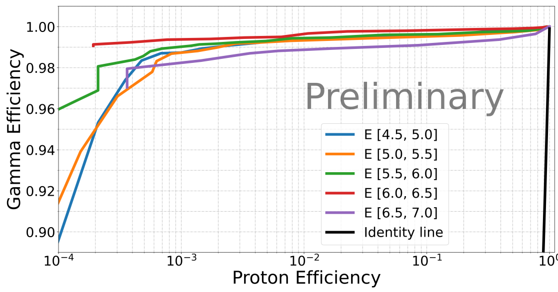


**(d)** Intermediate core bin.

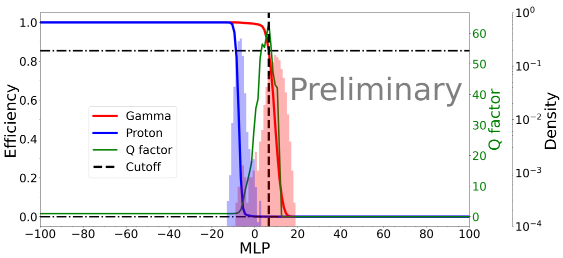


**(e)** Outer core bin.

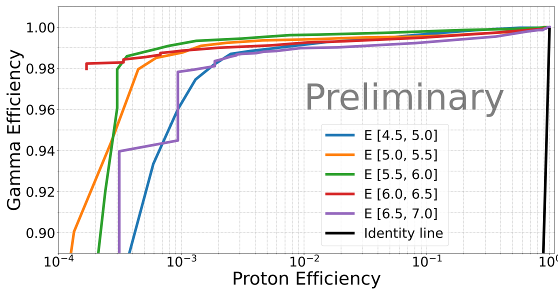


**(f)** Outer core bin.

**Figure 3:** The performance of the `MLP` is shown for three different bins corresponding to the central (top Figures, a & b), intermediate (middle Figures, c & d), and outer (bottom Figures, e & f) core bins. The Figures in the left column (using the same color and line definition as in Figure 1) display the `MLP` output distributions and efficiencies for events with logarithmic energies between 5.5 and 6.0. The Figures in the right column present the ROC curves of the `MLP` across five energy bins, following the same color scheme as Figure 1. These results demonstrate that combining multiple gamma/hadron separation observables significantly improves classification performance.

ten input parameters: seven gamma/hadron separation observables (`AFQ`, `DeepEASTER`, `GNN`, `LCm`, `LDFChi2`, `LHQ`, and `PINC`) and three additional reconstructed parameters (energy, zenith angle, and the distance between the shower core and the array center). An independent `MLP` model was trained for each bin using the ADAM optimizer, with an architecture of 10:12:12:1 (ten neurons in the input layer corresponding to the ten input parameters; two hidden layers with twelve neurons each; and one neuron in the output layer). The left column of Figure 3 shows the performance of three different trained models, where the `MLP` predictions for each event are presented as histograms, with their distributions clearly separated and minimal overlap. The right column presents the ROC curves for all bins analyzed in this contribution, with one Figure for each core bin showing curves for the five logarithmic energy bins. Although performance varies across energy and core bins, the `MLP` output consistently demonstrates excellent discrimination of proton events while retaining more than 80% of gamma events.

## 5. Discussion and Conclusions

A performance analysis of gamma/hadron separation was conducted using the full list of reconstructed observables available in the SWGO dataset. This analysis identified the most effective observables for this task. In Section 4, the three most powerful observables were reported, and their performance was shown to depend on energy and core position. The seven strongest gamma/hadron separation observables (`AFQ`, `DeepEASTER`, `GNN`, `LCm`, `LDFChi2`, `LHQ`, and `PINC`), together with three key shower parameters (energy, zenith angle, and distance from the core to the array center), were selected as inputs for the `MLP` model. An independent `MLP` model was trained for each bin to optimize the classification of detected particle events.

In this contribution, the first 15 bins corresponding to vertical events (zenith angles between 0° and 30°) were analyzed. The results demonstrate that the `MLP` models significantly outperform individual gamma/hadron separation observables. Although performance varies across energy and the core bins, the `MLP` models consistently achieve strong proton rejection while retaining more than 80% of gamma events. For example, the `MLP` performance for the logarithmic energy bin between 6.5 and 7.0 in the intermediate core bin (purple line in Figure 3c) is higher than that of the three best individual observables (purple line in the right column of Figure 1). This improvement is due to the `MLP` combining all input information to provide a better classification, which is why its ROC curve is closer to the ideal classifier.

## Acknowledgments

The SWGO Collaboration acknowledges the support from the agencies and organizations listed here https://www.swgo.org/SWGOWiki/doku.php?id=acknowledgements and from the following grants, ANID PIA/APOYO AFB230003; ANID/fondo 2022 quimal/Quimal220008; Center for Astrophysics and Associated Technologies (CATA; ANID Basal project FB210003); CONAHCYT CBF2023-2024-1630; CONCYTEC Project Fondecyt N078-202; CNPq Productivity Fellowship nr. 309053/2022-6; Croatian Science Foundation (HrZZ) Project IP-2022-10-4595; Czech Science Foundation 23-05827S; FAPERJ Fellowship "Cientista do Estado" nr. E-26/200.532/2023; FAPERJ Thematic Project nr. E-26/211.342/2021; FCT, under project PTDC/FIS-PAR/4300/2020; FONDECYT grant 1210131; GACR 23-05827S; National Research Foundation of Korea (RS-2023-00280210); National Research Foundation of Korea grants NRF-2023R1A2C2002751, NRF-2021R1A2C1094974; UNAM DGAPA-PAPIIT project number IG101323; UNSA-INVESTIGA (No. IBA-IB-35-2020-UNSA).

## References

[1] D.J. Fegan, *γ/hadron separation at TeV energies*, *J. Phys. G: Nucl. Part. Phys* **23** (1997) 1013.

[2] A. Abeysekara et al., *The High-Altitude Water Cherenkov (HAWC) observatory in México: The primary detector*, *Nucl. Instrum. Methods Phys. Res. A* **1052** (2023) 168253.

[3] F. Aharonian et al., *Performance of LHAASO-WCDA and observation of the Crab Nebula as a standard candle* *, *Chin. Phys. C* **45** (2021) 085002.

[4] A.U. Abeysekara et al., *The 2HWC HAWC Observatory Gamma-Ray Catalog*, *ApJ* **843** (2017) 40.

[5] A. Albert et al., *3HWC: The Third HAWC Catalog of Very-high-energy Gamma-Ray Sources*, *ApJ* **905** (2020) 76.

[6] A.U. Abeysekara et al., *Daily Monitoring of TeV Gamma-Ray Emission from Mrk 421, Mrk 501, and the Crab Nebula with HAWC*, *ApJ* **841** (2017) 100.

[7] R. Alfaro et al., *Gamma/hadron separation with the HAWC observatory*, *Nucl. Instrum. Methods Phys. Res. A* **1039** (2022) 166984.

[8] J. Li et al., *Application of Machine Learning to Background Rejection in Very-high-energy Gamma-Ray Observation*, *ApJS* **276** (2025) 24.

[9] I. Watson et al., *Deep Learning for the HAWC Observatory*, in *Proc. 38th Int. Cosmic Ray Conf. (ICRC2023)*, p. 927, July, 2023, DOI.

[10] R. Abbasi et al., *Graph Neural Networks for low-energy event classification &; reconstruction in IceCube*, *JINST* **17** (2022) P11003.

[11] J. Glombitza et al., *Application of graph networks to a wide-field water-Cherenkov-based Gamma-ray Observatory*, *JCAP* **2025** (2025) 066.

[12] SWGO Collaboration et al., *Science Prospects for the Southern Wide-field Gamma-ray Observatory: SWGO*, 2025. 10.48550/arxiv.2506.01786.

[13] A.U. Abeysekara et al., *Observation of the Crab Nebula with the HAWC Gamma-Ray Observatory*, *ApJ* **843** (2017) 39.

[14] A. Negro et al., *Expected performance of the SWGO observatory at Very High Energies (E> 30 TeV)*, in *Proc. 39th Int. Cosmic Ray Conf. (ICRC2025)*, July, 2025.

[15] R. Conceição et al., *Gamma/hadron discrimination at high energies through the azimuthal fluctuations of air shower particle distributions at the ground*, *JCAP* **2022** (2022) 086.

[16] M. Schneider et al., *Deep Learning Methods for Gamma/Hadron Separation in SWGO*, in *Proc. 39th Int. Cosmic Ray Conf. (ICRC2025)*, July, 2025.

[17] Y. Son et al., *Event Reconstruction Performance for SWGO using Attention-based Neural Network*, in *Proc. 39th Int. Cosmic Ray Conf. (ICRC2025)*, July, 2025.

# Full Author List: SWGO Collaboration

P. Abreu[1,2], R. Alfaro[3], A. Alfonso[4], M. Andrade[5], E. O. Angüner[6], E. A. Anita-Rangel[7], O. Aquines-Gutiérrez[8], C. Arcaro[9], R. Arceo[10], J. C. Arteaga-Velázquez[11], P. Assis[1,2], H. A. Ayala Solares[12], A. Bakalova[13], E. M. Bandeira[14], P. Bangale[12], U. Barres de Almeida[14,15], P. Batista[16], I. Batković[9,17], J. Bazo[18], E. Belmont[3], J. Bennemann[19], S. Y. BenZvi[20], A. Bernal[7], W. Bian[21], C. Bigongiari [22], E. Bottacini[9,17], R. Branada[23], P. Brogueira[1,2], A. M. Brown [64], T. Bulik[24], K. S. Caballero-Mora[10], P. Camarri[25,26], W. Cao[27], Z. Cao[27], Z. Cao[28], T. Capistrán[29,30], M. Cardillo[22], C. Casentini[22,25], C. Castromonte[31], P. M. Chadwick [64], J. Chanamé[32], J. Chang[28], S. Chen[21], A. Chiavassa[29,30], L. Chytka[13], R. Colalillo[33,34], R. Conceição[1,2], G. Consolati[35,36], R. Cordero[37], P. J. Costa[1,2], R. Covarelli[29,30], X. Cui[38], A. De Angelis[9,17], E. de Gouveia Dal Pino[39], R. de Menezes[14], P. Desiati[40], N. Di Lalla[85], F. Di Pierro[29,30], G. Di Sciascio[25], J. C. Díaz Vélez[40], C. Dib[23], B. Dingus[41,48], J. Djuvsland[19], C. Dobrigkeit [43], L. M. Domingues Mendes[1,44], T. Dorigo[9,45,46], M. Doro[9,17], A. C. dos Reis[14], M. Du Vernois[40], D. Elsaesser[47], K. Engel[48], T. Ergin[49,50], M. Errando[51], K. Fang[40], A. Fazzi[36,52], C. Feng[53], M. Feroci[22], C. N. Ferreira[54], N. Fraija[7], S. Fraija[7], A. Franceschini[17,83], G. F. Franco[14], S. Funk[16], R. Galleguillos[55], B. Gao[28], C. Gao[28], A. M. Garcia Reyes[7], S. Garcia[56], F. Garfias[7], G. Giacinti[21], L. Gibilisco[1,2], B. Giovanni [9,17], J. Glombitza[16], H. Goksu[19], G. Gong[57], B. S. González[1,2], M. M. González[7], J. Goodman[48], V. M. Grieco[34,58], M. Gu[28], F. Guarino[33,34], G. P. Guedes[59], J. Gyeong[60], F. Haist[19], G. Han[61], P. Hansen[62], J. P. Harding[41,42], S. Hernandez Cadena[21], I. Herzog[50], J. Hinton[19], W. Hofmann[19], C. Hou[28], Hou C.[28], K. Hu[53], D. Huang[48,63], P. Huentemeyer[63], A. Iriarte[7], J. Isaković[65], A. Jardin-Blicq[66,67], L. I. Junoy[68], J. Juryšek[13], S. Kaci[21], B. Khelifi[69], D. Kieda[70], F. La Monaca[22], G. La Mura[1,71], R. G. Lang[16], J. S. Lapington[72], R. Laspiur[73], L. Lavitola[34], J. Lee[74], F. Leitl[16], M. Lemoine-Goumard[66], L. Lessio [22], T. Lewis[63], C. Li[28], J. Li[27], K. Li[28], T. Li[21], B. Liberti[25], S. Lin[75], R. A. Lineros[68], D. Liu[53], J. Liu[28], R. Liu[76], F. Longo[77,78], Y. Luo[21], J. Lv[79], E. Macerata[36,52], G. Magugliani[36,52], K. Malone[41], A. Mancilla[80], D. Mandat[13], M. Manganaro[65], M. Mariani[36,52], A. Mariazzi[62], M. Mariotti[9,17], T. Marrodan[19], H. Martínez-Huerta[8], I. Martins[1,2], S. Medina[4], D. Melo[80], L. F. Mendes[1,2], E. Meza[81,82], R. Micali[5], D. Miceli[9,17], S. Miozzi[25], L. S. Miranda[5], P. E. Mirón Enriquez[7], A. Mitchell[16], A. Molinario[30,83], A. Montero[23], O. G. Morales-Olivares[10], A. Morselli[25], E. Mossini[36,52], M. Mostafá[12], F. Muleri[22], F. Nardi[9,17], A. P. Nayak[64], A. Negro[29,30], L. Nellen[84], M. Nisa[50], V. Novotny[13], L. Olivera-Nieto[19], N. Omodei[85], E. Orlando[77,78], S. Ortolani[17,83], M. Osorio-Archila[7], T. Ota[4], L. Otiniano[81], Z. Ou[21], A. Paoloni[86], I. M. Pepe[87], R. Perca[88], M. Peresano[29,30], Y. Pérez Araujo[7], T. Petrosillo-Lago[23], G. Piano[22], D. Piccolo[86], A. Pichel[89], M. Pimenta[1,2], M. Pirke[16], A. Porcelli[90], T. Porter[85], E. Prandini[9,17], A. Pratts[7], R. Pretsch[19], A. Qi[27], J. Qin[27], S. Rainò[91], L. Recabarren[9,17,92], M. Regeard[69], A. Reisenegger[93], Q. Remy[19], H. X. Ren[19], F. Rescic[65,94], B. Reville[19], M. Reyes[95], C. D. Rho[60], M. Riquelme[96], J. I. Rivadeneira[23], G. Rodriguez Fernandez[25], B. Rossi[34], A. C. Rovero[89], A. Ruina[9], E. Ruiz-Velasco[97], G. Salazar[73], C. Salotto[54], F. Sanchez[80], A. Sandoval[3], F. Sansone[33,34], M. Santander[98], R. Santonico[25,26], G. L. P. Santos[14], A. Santos-Guevara[8], D. Sartirana[30], M. Schneider[16], M. Schneider[48], H. Schoorlemmer[99], F. G. Schröder[19,102], H. Schutte[63], J. Serna-Franco[3], M. Shoaib[17], A. Smith[48], A. J. Smith[48], Y. Son[74], O. Soto[4], S. T. Spencer[16], R. W. Springer[70], J. Stewart[72], L. A. Stuani[101], H. Sun[53], M. Tambone[33,34], R. Tang[21], Z. Tang[27], S. Tapia[23], M. Tavani[22], R. Terrier[69], T. Terzić[65], K. Tollefson[50], B. Tomé[1,2], I. Torres[103], R. Torres-Escobedo[21], G. C. Trinchero[30,83], R. Turner[63], P. Ulloa[4], L. Valore[33,34], C. van Eldik[16], J. Vega[81], I. D. Vergara Quispe[62], A. Viana[5], J. Vícha[13], C. F. Vigorito[29,30], V. Vittorini[22], B. Wang[53], L. Wang[28], X. Wang[63], X. Wang[76], X. Wang[104], Z. Wang[21], Z. Wang[48], M. Waqas[33,34], I. J. Watson[74], F. Werner[19], R. White[19], C. Wiebusch[105], F. Wohlleben[19], S. Xi[28], G. Xiao[28], H. Xiao[21], L. Yang[75], R. Yang[27], Z. Yang[21], R. Yanyachi [88], Z. Yao[28], D. Zavrtanik[106], H. Zhang[21], H. Zhang[76], J. Zhang[38], S. Zhang[107], S. Zhang[50], X. Zhang[28], Y. Zhang[38], Y. Zhang[79], J. Zhao[28], L. Zhao[27], H. Zhou[21], C. Zhu[53], H. Zhu[38], P. Zhu[108], X. Zuo[28], P. Zyla[50],

[1]Laboratório de Instrumentação e Física Experimental de Partículas - LIP, Av. Prof. Gama Pinto, 2, 1649-003 Lisboa, Portugal, [2]Departamento de Física, Instituto Superior Técnico, Universidade de Lisboa, Av. Rovisco Pais 1, 1049-001 Lisboa, Portugal, [3]Instituto de Física, Universidad Nacional Autónoma de México, Circuito de la Investigación Científica, C.U., A. Postal 70-364, 04510 Cd. de México, México, [4]Universidad de La Serena, Chile, [5]Instituto de Física de São Carlos, Universidade de São Paulo, Av. Trabalhador São-carlense 400, São Carlos, Brasil, [6]TÜBİTAK Research Institute for Fundamental Sciences, 41470 Gebze, Turkey, [7]Instituto de Astronomía, Universidad Nacional Autónoma de México, Circuito Exterior, C.U., A. Postal 70-264, 04510 Cd. de México, México, [8]Departamento de Física y Matemáticas, Universidad de Monterrey, Av. Morones Prieto 4500, 66238, San Pedro Garza García NL, México, [9]INFN - Sezione di Padova, I-35131, Padova, Italy, [10]Facultad de Ciencias en Física y Matemáticas, Universidad Autónoma de Chiapas, C. P. 29050, Tuxtla Gutiérrez, Chiapas, México, [11]Instituto de Física y Matemáticas, Universidad Michoacana de San Nicolás de Hidalgo, Morelia, Michoacan, Mexico, [12]Temple University , Dept. of Physics, Philadelphia, PA, USA, [13]Institute of Physics of the Czech Academy of Sciences, Prague, Czech Republic, [14]Centro Brasileiro de Pesquisas Físicas (CBPF), Rua Dr. Xavier Sigaud 150, 22290-180 Rio de Janeiro, Brasil, [15]Universidade de São Paulo, Instituto de Astronomia, Geofísica e Ciências Atmosféricas, Departamento de Astronomia, Rua do Matão 1226, 05508-090 São Paulo, Brasil, [16]Friedrich-Alexander-Universität Erlangen-Nürnberg, Erlangen Centre for Astroparticle Physics, Nikolaus-Fiebiger-Str. 2, D 91058 Erlangen, Germany, [17]Università di Padova, I-35131, Padova, Italy, [18]Pontificia Universidad Católica del Perú, Av. Universitaria 1801, San Miguel, 15088, Lima, Perú, [19]Max-Planck-Institut für Kernphysik, Saupfercheckweg 1, 69117 Heidelberg, Germany, [20]Department of Physics and Astronomy, University of Rochester, Rochester, NY, USA, [21]Tsung-Dao Lee Institute & School of Physics and Astronomy, Shanghai Jiao Tong University, 520 Shengrong Road, Shanghai 201210, China, [22]Istituto Nazionale di Astrofisica - Istituto di Astrofisica e Planetologia Spaziali (INAF-IAPS), Via del

Fosso del Cavaliere 100, 00133, Roma, Italy, [23]CCTVal, Universidad Tecnica Federico Santa Maria, Chile, [24]Astronomical Observatory Warsaw University, 00-478 Warsaw, Poland, [25]INFN, Roma Tor Vergata, Italy, [26]Department of Physics, University of Roma Tor Vergata, Viale della Ricerca Scientifica 1, I-00133 Roma, Italy, [27]School of physical science, University of Science and Technology of China, 96 Jinzhai Road, Hefei, Anhui 230026, China, [28]Institute of High Energy Physics, Chinese Academy of Science, 19B Yuquan Road, Shijingshan District, Beijing 100049, China, [29]Università degli Studi di Torino, I-10125 Torino, Italy, [30]INFN, Sezione di Torino, Torino, Italy, [31]Universidad Nacional de Ingeniería, Av. Túpac Amaru 210 - Rímac. Apartado 1301, Lima Perú, [32]Instituto de Astrofísica, Pontificia Universidad Católica de Chile (PUC), Av. Vicuña Mackenna 4860, 782-0436, Macul, Santiago, Chile, [33]Università di Napoli "Federico II", Dipartimento di Fisica "Ettore Pancini", Napoli, Italy, [34]INFN, Sezione di Napoli, Napoli, Italy, [35]Politecnico di Milano, Dipartimento di Scienze e Tecnologie Aerospaziali, Milano, Italy, [36]INFN, sezione di Milano, Milano, Italy, [37]Departamento de Física, Universidad de Santiago de Chile, Chile, [38]National Astronomical Observatories, Chinese Academy of Sciences (NAOC, CAS), China, [39]Universidade de São Paulo, São Paulo, Brasil, [40]Wisconsin IceCube Particle Astrophysics Center (WIPAC) & Department of Physics, [41]Los Alamos National Laboratory, Los Alamos, NM, USA, [42]New Mexico Consortium, Los Alamos, NM, USA, [43]Departamento de Raios Cósmicos e Cronologia, Instituto de Física "Gleb Wataghin", Universidade Estadual de Campinas, C.P. 6165, 13083-970 Campinas, Brasil, [44]Centro Federal de Educação Tecnológica Celso Suckow da Fonseca (CEFET), Rio de Janeiro, Brasil, [45]Luleä University of Technology, Laboratorievägen 14, SE-971 87 LULEÅ, Sweden, [46]Universal Scientific Education and Research Network, Italy, [47]Technische Universität Dortmund, D-44221 Dortmund, Germany, [48]Department of Physics, University of Maryland, College Park, MD, USA, [49]Middle East Technical University, Northern Cyprus Campus, 99738 Kalkanli via Mersin 10, Turkey, [50]Department of Physics and Astronomy, Michigan State University, East Lansing, MI, USA, [51]Department of Physics, Washington University in St Louis, St Louis, MO 63130, USA, [52]Politecnico di Milano, Dipartimento di Energia, Milano, Italy, [53]Key Laboratory of Particle Physics and Particle Irradiation (MOE), Institute of Frontier and Interdisciplinary Science, Shandong University, Qingdao, Shandong 266237, China, [54]Instituto Federal de Educação, Ciência e Tecnológia Fluminense 28030-130 Campos, RJ, Brazil, [55]Universidad Finis Terrae, Chile, [56]Universidad Nacional de San Antonio Abad del Cusco, Av. de la Cultura, Nro. 733, Cusco - Perú, [57]Dept. of Engineering Physics, Tsinghua University, 1 Tsinghua Yuan, Haidian District, Beijing 100084, China, [58]Scuola Superiore Meridionale, Napoli, Italy, [59]Universidade Estadual de Feira de Santana, Feira de Santana, Brazil, [60]Department of Physics, Sungkyunkwan University, Suwon, South Korea, [61]School of Mechanical Engineering and Electronic Information, China University of Geosciences, Wuhan, Hubei 430074, China, [62]IFLP, Universidad Nacional de La Plata and CONICET, La Plata, Argentina, [63]Michigan Technological University, Houghton, Michigan, 49931, USA, [64]Department of Physics, Durham University, South Rd, Durham DH1 3LE, United Kingdom, [65]University of Rijeka, Faculty of Physics, 51000 Rijeka, Croatia, [66]Univ. Bordeaux, CNRS, LP2i Bordeaux, UMR 5797, F-33170 Gradignan, France, [67]French-Chilean Laboratory for Astronomy, IRL 3386, CNRS and Universidad de Chile, Casilla 36-D, Santiago, Chile, [68]Departamento de Física, Universidad Católica del Norte, Avenida Angamos 0610, Casilla 1280, 1270709 Antofagasta, Chile., [69]Université Paris Cité, CNRS, Astroparticule et Cosmologie, F-75013 Paris, France, [70]Department of Physics and Astronomy, University of Utah, Salt Lake City, UT, USA, [71]INAF - Osservatorio Astronomico di Cagliari, Via della Scienza 5, 09047 Selargius, Italy, [72]University of Leicester, School of Physics and Astronomy, University Road, Leicester, LE1 7RH, United Kingdom, [73]Facultad de Ciencias Exactas, Universidad Nacional de Salta, Avda. Bolivia 5150, A4408FVY, Salta, Argentina, [74]University of Seoul, Seoul, Rep. of Korea, [75]School of Physics and Astronomy, Sun Yat-sen University, Zhuhai, Guangdong 519082, China, [76]School of Astronomy and Space Science, Nanjing University, Xianlin Avenue 163, Qixia District, Nanjing, Jiangsu 210023, China, [77]Dipartimento di Fisica, Università degli Studi di Trieste, via Valerio 2, I-34127 Trieste, Italy, [78]INFN - Sezione di Trieste, via Valerio 2, I-34127 Trieste, Italy, [79]Aerospace Information Research Institute, Chinese Academy of Science, 9 Dengzhuang South Road, Haidian District, Beijing 100094, China, [80]Instituto de Tecnologías en Detección y Astropartículas (CNEA, CONICET, UNSAM), Buenos Aires, Argentina, [81]Comisión Nacional de Investigación y Desarrollo Aeroespacial, Calle Luis Felipe Villarán 1069, 15046, Lima, Perú, [82]Universidad Nacional de Moquegua, Calle Ancash SN, 18001, Moquegua, Perú, [83]Instituto Nazionale Di Astrofisica (INAF), Torino, Italy, [84]Instituto de Ciencias Nucleares, Universidad Nacional Autónoma de México, Circuito Exterior, C.U., A. Postal 70-543, 04510 Cd. de México, México, [85]Standford University, USA, [86]Laboratori Nazionali di Frascati INFN, Italy, [87]Universidade Federal da Bahia, Brasil, [88]Universidad Nacional de San Agustin de Arequipa, Santa Catalina Nro. 117. Arequipa, Perú, [89]Instituto de Astronomía y Física del Espacio (IAFE (CONICET-UBA)), Ciudad Universitaria, CABA, Argentina, [90]Centro de Astronomía (CITEVA), Universidad de Antofagasta, Chile, [91]Università degli Studi di Bari Aldo Moro, Italy, [92]Centro di Ateneo di Studi e Attività Spaziali "Giuseppe Colombo", Via Venezia 15, I-35131 Padova, Italy., [93]Departamento de Física, Facultad de Ciencias Básicas, Universidad Metropolitana de Ciencias de la Educación, Av. José Pedro Alessandri 774, Ñuñoa, Chile, [94]Departamento de Física Teórica, Universidad de Zaragoza, Zaragoza 50009, Spain, [95]Universidad del Bío-Bío, Chile, [96]Universidad de Chile, Chile, [97]Université Savoie Mont Blanc, CNRS, Laboratoire d'Annecy de Physique des Particules—IN2P3, F-74000 Annecy, France, [98]Department of Physics and Astronomy, University of Alabama, Tuscaloosa, Alabama, 35487, USA, [99]IMAPP, Radboud University Nijmegen, Nijmegen, The Netherlands, [100]IRFU, CEA, Université Paris-Saclay, F-91191 Gif-sur-Yvette, France, [101]Unidade Acadêmica de Física, Universidade Federal de Campina Grande, Av. Aprígio Veloso 882, CY2, 58.429-900 Campina Grande, Brasil, [102]Bartol Research Institute, Department of Physics and Astronomy, University of Delaware, Newark, DE, USA, [103]Instituto Nacional de Astrofísica, Óptica y Electrónica, Puebla, Mexico, [104]School of Integrated Circuit, Ludong University, 186 Hongqi Middle Road, Zhifu District, Yantai, Shandong, China, [105]RWTH Aachen University, Templergraben 55, 52062 Aachen, Germany, [106]Center for Astrophysics and Cosmology (CAC), University of Nova Gorica, Nova Gorica, Slovenia, [107]College of Engineering, Hebei Normal University, 20 South Second Ring East Road, Shijiazhuang, Hebei, China, [108]School of mechanical engineering, University of Science and Technology Beijing, 30 Xueyuan Road, Haidian District, Beijing 100083, China,

PoS(ICRC2025)593